Acta Crystallographica Section D
Biological Crystallography
ISSN 0907-4449

Crystallization and preliminary X-ray analysis of the catalase–peroxidase KatG from *Burkholderia pseudomallei*

Xavier Carpena,[a] Jack Switala,[b] Suvit Loprasert,[c] Skorn Mongkolsuk,[c] Ignacio Fita[a] and Peter C. Loewen[b]*

[a]Institut de Biología Molecular de Barcelona CSIC, Jordi-Girona 18-26, 08034 Barcelona, Spain, [b]Department of Microbiology, University of Manitoba, Winnipeg, MB, R3T 2N2, Canada, and [c]Laboratory of Biotechnology, Chulabhorn Research Institute, Lak Si, Bangkok 10210, Thailand

Correspondence e-mail: peter_loewen@umanitoba.ca

Received 26 June 2002
Accepted 30 September 2002

The bifunctional catalase–peroxidase KatG encoded by the *katG* gene of *Burkholderia pseudomallei* has a predicted subunit size of 81.6 kDa. It shows high sequence similarity to other catalase–peroxidases of bacterial, archaebacterial and fungal origin, including 64% identity to KatG from *Mycobacterium tuberculosis* and lesser sequence similarity to members of the plant peroxidase family. Crystals from this protein were grown in 16–20% PEG 4000, 20% 2-methyl-2,4-pentanediol and 0.1 *M* sodium citrate pH 5.6 by the hanging-drop vapour-diffusion method at 293 K. These crystals diffracted beyond 1.8 Å resolution and belong to space group $P2_12_12_1$, with unit-cell parameters a = 100.9, b = 115.6, c = 175.2 Å. The data are consistent with either a monomer or a dimer in the crystal asymmetric unit.

1. Introduction

The bifunctional catalase–peroxidases (CPx) are found in a wide variety of organisms including bacteria, archaebacteria and fungi (Nicholls *et al.*, 2001). They are protective enzymes that degrade hydrogen peroxide either catalatically ($2H_2O_2 \rightarrow 2H_2O + O_2$) or peroxidatically ($H_2O_2 + 2AH \rightarrow 2H_2O + 2A^{\cdot}$), thereby preventing hydroxyl-radical-induced cellular damage. The rapidity of the catalatic reaction results in the catalase–peroxidases appearing to be predominantly catalases, despite their sequences suggesting a close relation to the plant peroxidases. Indeed, the close relation to the plant peroxidases was confirmed when the Trp105Phe variant of *Escherichia coli* HPI (hydroperoxidase I) proved to be a predominant peroxidase, with a 1000-fold lower catalatic activity and a three-fold higher peroxidatic activity (Hillar *et al.*, 2000).

The catalase–peroxidases gained significant notoriety in 1992 when it was confirmed that mutation of the *katG* gene encoding the *Mycobacterium tuberculosis* catalase peroxidase imparted isoniazid resistance (Zhang *et al.*, 1992). Given the importance of isoniazid as an anti-tuberculosis drug and the prevalence of *katG*-induced resistance, interest in determining the structure of KatG grew, with several groups worldwide attempting to solve its structure. Unfortunately, attempts to crystallize a number of different catalase–peroxidases were without success until very recently, when the crystallization of the enzymes from *Haloarcula marismortui* (Yamada *et al.*, 2001) and *Synechococcus* (Wada *et al.*, 2002) and of the C-terminal domain of *E. coli* HPI were reported (Carpena *et al.*, 2002).

The large size of the CPx subunits, which contains two distinct sequence-related domains, relative to the plant peroxidases may have been the result of a gene duplication and fusion event (Welinder, 1991). The N-terminal domain is the active domain, containing haem and active-site residues that when modified affect enzyme activity. The C-terminal domain has less sequence similarity, does not seem to bind haem and does not have the well conserved active-site motif characteristic of peroxidases. The haem occupancy for many catalase–peroxidases is partial, with an average of 0.5 haem per subunit in a heterogeneous mixture of dimers and tetramers with 0, 1 and 2 or 1, 2 and 3 haems, respectively (Hillar *et al.*, 2000). In this paper, we report that the CPx from *Burkholderia pseudomallei* (*Bp*CPx) purifies with an apparently higher haem-to-subunit ratio. This more homogeneous protein proved amenable to rapid crystallization and the crystals diffracted to 1.8 Å.

2. Experimental results

2.1. Protein purification and characterization

The plasmid pBG306 was constructed by inserting a 3.0 kbp *Sma*I–*Sfi*I fragment containing the *B. pseudomallei katG* open reading frame (GenBank Accession No.

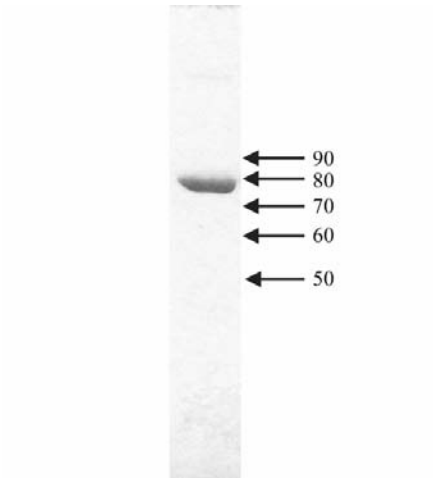

Figure 1
Purified *Bp*CPx separated on a 10% SDS polyacrylamide gel. The arrows indicate the location of size markers (values are in kDa).

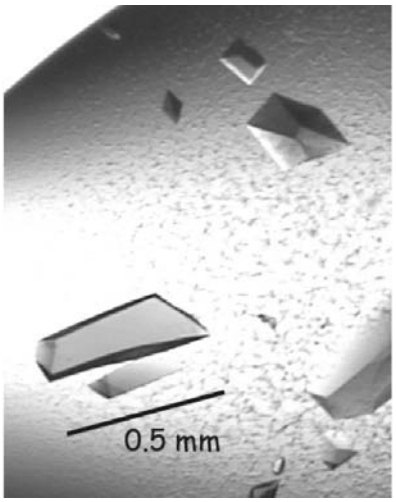

Figure 2
Orthorhombic crystals of *B. pseudomallei* KatG (*Bp*CPx).

AY040244) into the plasmid pBBR-*Cm* (Kovach & Elzer, 1995) and transforming into UM262 (Loewen *et al.*, 1990). Cultures were grown with shaking in LB medium supplemented with 4 μg ml^{-1} chloramphenicol and 40 μg ml^{-1} haem (Sigma) for 16 h at 301 K. Following harvesting, the cells were lysed using a French press. *Bp*CPx was purified by fractionation with streptomycin sulfate, ammonium sulfate, elution from DEAE cellulose with a linear gradient of 0–0.5 *M* NaCl and elution from hydroxylapatite with a linear gradient of 5–200 m*M* potassium phosphate pH 7. The purified protein presented a single band on a denaturing SDS polyacrylamide gel (Fig. 1) and stained for both catalatic and peroxidatic activities on a non-denaturing gel (not shown). The catalase specific activity was 2200 units per milligram of protein (one unit of catalase decomposes 1 μ*M* of H_2O_2 in 1 min at 310 K) and the final A_{407}/A_{280} ratio was 0.60.

2.2. Crystallization and data collection

Initially, Hampton Crystal Screen 1 and 2 kits were used for screening; after optimization, thin tetragonal crystal plates were obtained from purified *Bp*CPx within 3–5 d at 293 K using the hanging-drop diffusion method with 1 μl of a 22 mg ml^{-1} protein solution and 1 μl of reservoir solution containing 16–20% PEG 4K, 20% MPD and 0.1 *M* sodium citrate pH 5.6. These crystals yielded low-resolution data when collected using a home radiation source, which allowed their characterization as tetragonal with unit-cell parameters a = 177, b = 177, c = 99 Å. A second crystal form, consisting of brownish parallelepiped-shaped crystals reaching 0.5 × 0.2 × 0.2 mm in size (Fig. 2), was also obtained in a few days under identical crystallization conditions but with a higher protein-to-reservoir solution ratio, being prepared with 1 μl reservoir solution and 2 μl 22 mg ml^{-1} protein solution. Crystals from this second form diffracted beyond 1.9 Å resolution when using a synchrotron source. The unit cell, characterized using 1° rotation diffraction images, was consistent with the primitive orthorhombic space group $P2_12_12_1$, with unit-cell parameters a = 100.9, b = 115.6, c = 175.2 Å. A data set was collected from a single flash-cooled crystal at the BM7B beamline of the DESY Hamburg Outstation on a MAR Research imaging-plate detector using radiation of 0.85 Å wavelength (Fig. 3). Diffraction data were indexed and integrated using the program *DENZO* and merged using the program *SCALEPACK* (Otwinowski & Minor, 1996) (Table 1).

The self-rotation function calculated using the program *MOLREP* (Vagin & Teplyakov, 1997) did not show significant peaks besides those corresponding to the crystallographic twofold axis. In turn, native Patterson maps calculated using the *CCP*4 package (Collaborative Computational Project, Number 4, 1994) proved the absence of translational symmetries. Therefore, the orthorhombic *Bp*CPx crystals appear to contain only one protein subunit in the crystal asymmetric unit, which would correspond to a volume solvent content percentage of 80% (Matthews coefficient 6.26 Å^3 Da^{-1}). However, a non-crystallographic twofold axis in a direction almost parallel (within a few degrees) to one of the crystallographic twofold axis could still exist and be undetected by both the self-rotation and native Patterson. Two subunits in the crystal asymmetric unit would correspond to a 60% solvent content (Matthews coefficient 3.13 Å^3 Da^{-1}) and would be compatible with the existence of a molecular dimer. The possibility of molecular tetramers seems incompatible with the present crystal packing analysis.

Table 1
Data-collection statistics.

Values in parentheses are for the highest resolution shell.

Space group	$P2_12_12_1$
Resolution (Å)	1.8
Unit-cell parameters (Å)	a = 100.9, b = 115.6, c = 175.2
No. of measured reflections	663193
No. of unique reflections	186738 (9316)
Completeness (%)	99.0 (99.9)
$R_{\rm merge}$† (%)	6.4 (46.4)
Average $I/\sigma(I)$	20.2 (2.9)
Mosaicity	0.3

† $R_{\rm merge} = \sum|I_i - \langle I\rangle|/\sum(I_i)$.

Crystal structure determination is now in progress by molecular replacement using the programs *AMoRe* (Navaza, 1994) and *BEAST* (Read, 2001). Search models for the N-terminal region of *Bp*CPx have been derived from yeast cytochrome *c* peroxidase (Finzel *et al.*, 1984). Search models for the C-terminal region of *Bp*CPx have been

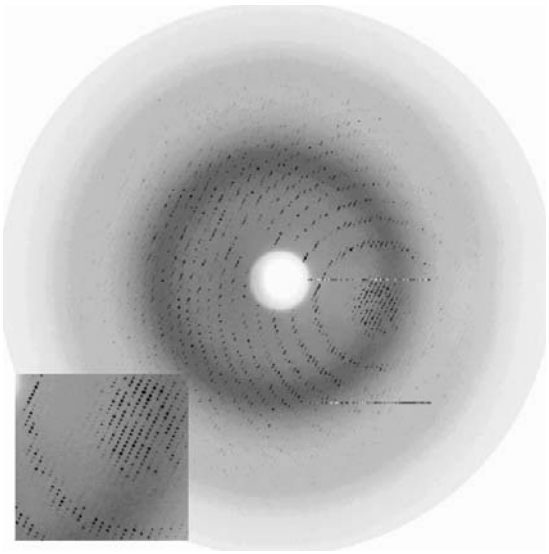

Figure 3
Diffraction image, collected at BM7B in DESY (Hamburg), from an orthorhombic crystal of *Bp*CPx. The image edge, where faint spots are still visible, corresponds to a resolution of 1.58 Å.

derived from the results from crystals of KatG_2D from *E. coli* HPI (Carpena *et al.*, 2002; Carpena *et al.*, unpublished results).

3. Conclusions

The catalase–peroxidase from *B. pseudomallei* has been crystallized from sodium citrate pH 5.6 and the crystals diffract beyond 1.8 Å. The diffraction data is well suited to high-resolution studies, which are in progress. The data is compatible with either one subunit in the crystal asymmetric unit, corresponding to solvent content of 80%, or to a dimer of subunits, corresponding to a solvent content of 60%.

This work was supported by grants BIO099-0865 from DGICYT to IF and OGP9600 from the Natural Sciences and Engineering Research Council of Canada (NSERC) to PCL.

References

Carpena, X., Guarné, A., Ferrer, J. C., Alzari, P. M., Fita, I. & Loewen, P. C. (2002). *Acta Cryst.* D**58**, 853–855.
Collaborative Computational Project, Number 4 (1994). *Acta Cryst.* D**50**, 760–763.
Finzel, B. C., Poulos, T. L. & Kraut, J. (1984). *J. Biol. Chem.* **259**, 13027–13036.
Hillar, A., Peters, B., Pauls, R., Loboda, A., Zhang, H., Mauk, A. G. & Loewen, P. C. (2000). *Biochemistry*, **39**, 5868–5875.
Kovach, M. E. & Elzer, P. H. (1995). *Gene*, **166**, 175–176.
Loewen, P. C., Switala, J., Smolenski, M. & Triggs-Raine, B. L. (1990). *Biochem. Cell Biol.* **68**, 1037–1044.
Navaza, J. (1994). *Acta Cryst.* A**50**, 157–163.
Nicholls, P., Fita, I. & Loewen, P. C. (2001). *Adv. Inorg. Chem.* **51**, 51–106.
Otwinowski, Z. & Minor, W. (1996). *Methods Enzymol.* **276**, 307–326.
Read, R. J. (2001). *Acta Cryst.* D**57**, 1373–1382.
Vagin, A. & Teplyakov, A. (1997). *J. Appl. Cryst.* **30**, 1022–1025.
Wada, K., Tada, T., Nakamura, Y., Kinoshita, T., Tamoi, M., Sigeoka, S. & Nishimura, K. (2002). *Acta Cryst.* D**58**, 157–159.
Welinder, K. (1991). *Biochim. Biophys. Acta*, **1080**, 215–220.
Yamada, Y., Saijo, S., Sato, T., Igarashi, N., Usui, H., Fujiwara, T. & Tanaka, N. (2001). *Acta Cryst.* D**57**, 1157–1158.
Zhang, Y., Heym, B., Allen, B., Young, D. & Cole, S. (1992). *Nature (London)*, **358**, 591–593.